Retinal Signalling

Changing dynamics of spontaneous waves during retinal development: a novel panretinal perspective achieved with the Active Pixel Sensor (APS) 4,096 electrodes array

Evelyne Sernagor[1*], Alessandro Maccione[2], Matthias H. Hennig[3], Mauro Gandolfo[4], Stephen J. Eglen[5], Luca Berdondini[2]

1 Institute of Neuroscience, Newcastle University Medical School, Newcastle upon Tyne, UK
2 Department of Neuroscience and Brain Technologies, Italian Institute of Technology, Genova, Italy
3 Institute for Adaptive and Neural Computation, School of Informatics, University of Edinburgh, Edinburgh, UK
4 Department of Biophysical and Electronic Engineering, University of Genova, Genova, Italy
5 Department of Applied Mathematics and Theoretical Physics, Cambridge University, Cambridge, UK
* Corresponding author. E-mail address: evelyne.sernagor@ncl.ac.uk

Keynote Lecture

The developing retina exhibits spontaneous waves of activity spreading across the ganglion cell layer. These waves are present only during a limited perinatal period, and they are known to play important roles during the wiring of visual connections. Using the APS MEA devices consisting of 4,096 electrodes recording at near cellular resolution, we have been able to achieve panretinal recordings of retinal waves in the neonatal mouse retina. We found that the spatiotemporal patterns of the waves undergo profound developmental changes as retinal synaptic networks mature, switching from slow random events propagating over large retinal areas to faster, spatially more restricted events, following several clear repetitive, non-random propagation patterns. This novel panretinal perspective of wave dynamics provides new clues about the role played by retinal waves during visual map formation.

1 Introduction

During perinatal development, neighboring retinal ganglion cells (RGCs) fire in correlated bursts of action potentials, resulting in waves spreading across the RGC layer (for review see [1,2]). These waves, discovered nearly two decades ago using a multielectrode array (MEA) recording from the RGC layer [3], have been the subject of intense investigation to understand their generation and propagation mechanisms and to decipher their role during the wiring of retinal projections (for review see [2]). Retinal waves have been investigated with MEAs ranging from 60 [2 for review] to 512 electrodes [4] (sampling limited by the distance between electrodes) or with Ca^{2+} imaging [1,2] (sampling limited by the low temporal resolution of Ca^{2+} indicators). With either approach, only a limited window of the retina can be sampled at any given time, and wave dynamics have been extrapolated from these spatially restricted windows. In the mammalian retina, the earliest waves propagate through gap junctions (Stage I) [2,5], followed by propagation through lateral connections between cholinergic starburst amacrine cells (Stage II) [2,6]. Finally, once glutamatergic connections mature and RGCs become driven by light, retinal waves switch from cholinergic to glutamatergic control (Stage III) [2,5,7] before they disappear completely. Despite these major developmental changes in network connectivity, it is still unclear to what extent wave dynamics change with development. The spatiotemporal wave patterns are hypothesised to provide cues for the establishment of retinal receptive fields and for the binocular organisation and visual map formation in retinal targets. In this study, we have used the APS MEA [8,9] to record retinal waves from the neonatal mouse at P1-P5 (Stage II) and at P9-11 (Stage III). The 64x64 APS MEA records at near cellular resolution (21x21μm electrodes, 21μm separation), where all channels can be acquired at high enough temporal resolution (7.8 kHz/channel for full frame acquisition) to detect single spike signals reliably. The channels are integrated over an active area of 2.67x2.67 mm, which is large enough to cover most of the neonatal mouse retina (see Fig. 1A). Hence, with its large size and unprecedented spatiotemporal resolution, the APS MEA provides the ideal experimental tool to investigate developmental changes in retinal waves dynamics.

2 Materials and methods

This study was done using C57b1/6 neonatal mice. Mouse pups were killed by cervical dislocation

and enucleated before retinal isolation. The isolated retina was then transferred to the experimental chamber and placed, RGC layer facing down, onto 64x64 MEAs [8,9]. Better coupling between the tissue and the electrodes was achieved by placing a small piece of polyester membrane filter (5 µm pores) on the retina followed by a custom made slice anchor holder. The retina was kept at 32°C and continuously perfused (2 ml/min) with artificial cerebrospinal fluid containing the following (in mM):118 NaCl, 25 $NaHCO_3$, 1 NaH_2PO_4, 3 KCl, 1 $MgCl_2$, 2 $CaCl_2$, and 10 glucose, equilibrated with 95% O_2 and 5% CO_2. The retina was usually left for 30-60 min to settle on the MEA before starting the recording, allowing time for coupling to improve and for spontaneous activity to develop.

Electrophysiological signals were acquired from the whole array at 7.8 kHz sampling rate and visualized on screen during recordings. Successively, off-line spike detection was performed by using a recently presented Precise Timing Spike Detection (PTSD) algorithm [10] since it enables a fast and precise identification of the spike events..

Spike trains were used to generate raster plots and activity maps using BrainWave as well as custom designed codes written in Matlab and R.

3 Results

We have investigated the spatiomporal properties of retinal waves at P1,2,3,4,5 (Stage II) and P9,10,11 (Stage III). For the youngest animals, the entire retina fits on the MEA, and it is even smaller than the active area of the electrodes (2.67x2.67mm). Figure 1A shows a P10 retina on the MEA. The photograph was taken at the end of the recording session, after removal of the anchor and filter paper. In this case, the outer peripheral retina is beyond the limits of the active area. A map of the active electrodes during a 10 minutes recording session is overlayed on the retina. The colours indicate the log of the firing rate on each electrode (see Figure 3 for more details on activity maps). There is no activity at the centre, mostly around the optic disk (red circle), a feature we have observed in most retinas. In this particular retina, there was virtually no activity on the bottom left and left side of the tissue. The lack of activity along the left side was probably due to poor coupling (as verified at the end of the experiment). However, based on visual inspection, the coupling seemed strong in the bottom left part of the MEA, but nevertheless that part of the retina had very little spontaneous activity.

Figure 1B shows an activity raster plot recorded over 15s in the same retina. There were 1180 active channels during that same period. The raster plots (arranged by electrode rows) show complex propagation patterns across the tissue. However, a 2 dimensional view of the activity is necessary to visualise these patterns. This is shown in time lapse single frames of activity raw data taken at 342, 344, 347, 352 and 354 s. The colour map represents the electrical activity variance calculated over a 0.5s time window. Three clear waves in distinct parts of the array are apparent over the recording period. Figure 1B also illustrates raw data from selected channels scattered across the right side of the array. These channels were active during the network bursts, showing clear activity propagation between them.

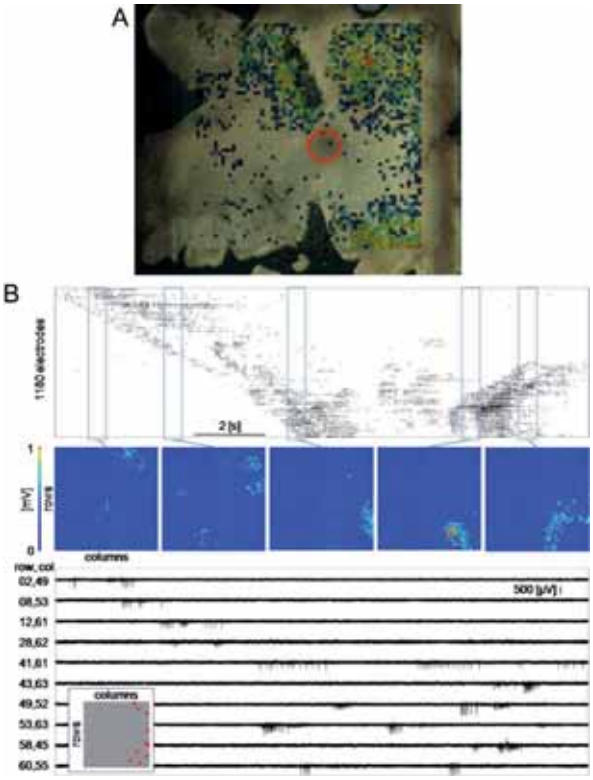

Fig. 1. Spontaneous activity in a P10 retina. **A**: photograph of the retina on the MEA, acquired at the end of the recording session. The overlay represents the map of the activity recorded during a 10 min trial. Dots are colour coded for the log of the firing rate (see fig. 3 for more details). **B:** Activity recorded over 15 s in the same retina. The top panel illustrates the raster plot of the activity, with the channels arranged according to rows on the MEA. The middle panel shows time lapse images of the activity as it propagates across the retina during the same 15 s. See text for more details. The bottom panel shows the raw data for 10 channels selected within the path of the activity on the right side of the array.

Starburst amacrine cholinergic connections initially drive the waves. However, the wave-generation synaptic network undergoes profound changes around P9, when RGCs become driven by light, at the time of the maturation of bipolar glutamatergic connections. Despite these fundamental changes in the network

driving retinal waves, no consistent differences between Stage II and Stage III wave dynamics have been reported in the literature. Experimental limitations due to the relatively small spatial windows in 60 channels MEA recordings, or to the poor temporal resolution in imaging experiments, may indeed prevent achieving a clear overview of perhaps subtle (but nevertheless important from a functional point of view) global wave dynamics changes. With the APS MEA, we have observed fundamental differences in the spatiotemporal properties of Stage II and III waves. Figure 2 illustrates raster plots of spontaneous activity recorded at P4-5 (Stage II) and P9 and P11 (Stage III). In the P4 and P5 retinas, waves are initiated in random locations and they slowly propagate across large retinal areas. At Stage III, however, the waves are often, but not always, spatially more restricted, as clearly revealed in the raster plots. Indeed, most episodes of activity appear to recruit only a limited subset of the RGC population. Another clear difference is that the waves appear to propagate much faster at these later stages.

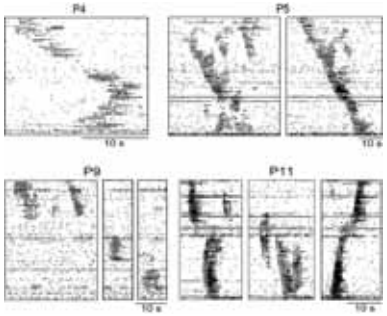

Fig. 2. Raster plots of spontaneous activity at different developmental stages.

Figure 3 provides information on the spatial distribution of the spontaneous activity at these different stages. The figure illustrates activity maps computed over 10 min trials. The dots on the plots represent active electrodes, and the colours of the dots reflect the average firing rate (calculated in log spikes/s) for these channels. At P4, the activity appears completely scattered across the retina, with no distinct patterns of spatial organisation. At P5, the activity is stronger and perhaps slightly more clustered, but still with no clear spatial patterns. At P9, on the other hand, when glutamatergic connections take over from acetylcholine in controlling the waves, the activity becomes clustered in small areas on the array (inspection after the recording session revealed that there was no retina on the right side of the MEA). These clusters appear to tile the retina in a non-overlapping manner. The activity becomes stronger at P10-11, but even so, it appears clustered in the same specific retinal areas rather than propagating across the entire tissue like at Stage II. Interestingly, Stage II waves are initiated at random locations, both in the center and in the periphery, whereas at Stage III, waves appear to be mostly generated in the periphery and they propagate towards the central retina.

The maturation of GABAergic inhibition is known to play an important role in retinal wave dynamics, causing them to become smaller and more static until they completely disappear [2,5,11]. Hence, GABA may be responsible for the emergence of the ativity clusters at Stage III. In the P9 retina illustrated in Figure 3, upon addition of bicuculline (10 μM), a $GABA_A$ receptor antagonist, the activity became stronger and two new clusters emerged (Figure 3).

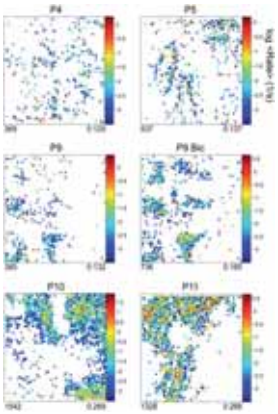

Fig. 3. Spontaneous activity maps computed over the entire MEA during 10 minutes recording sessions at different developmental stages. The activity is colour coded following the log of the firing rate (spikes/s). Left bottom corner number: total number of active channels. Right bottom corner number: average firing rate.

Nevertheless, the activity remained clustered and it did not start to propagate over large retinal areas. $GABA_A$ blockade results in significantly longer bursts and faster wave propagation, as clearly illustrated in the raster plots of Figure 4, suggesting that synaptic inhibition dampens propagation across the network. In addition, in the presence of bicuculline, the activity sometimes seems to "flow" more easily between clusters, such as between the two clusters on the right side of the array at P10 in Figure 3. The top raster plot in Figure 4 represents spontaneous activity in that area of the P10 retina in control condition. The wave front, outlined by the red arrow, clearly shows how activity comes to an almost complete stop in the middle of the episode. In the presence of bicuculline, the activity becomes not only faster, but on occasion, it also succeeds in propagating smoothly from one area to the other (bottom raster plot). However, it is important to point out that in many other episodes, these clusters

remain clearly separated, and often do not occur consecutively.

4 Discussion and concluding remarks

In this study, we have demonstrated that the APS MEA is a powerful tool to investigate the spatiotemporal behaviour of developing retinal networks. Indeed, we have achieved new insights about developmental changes in wave dynamics, during the critical period for wiring of the visual system. Stage II waves are slow and wide spreading in the retina, propagating with a high degree of randomness whereas Stage III are faster and spatially more restricted. Previous studies in chick [12] and turtle [11] (where both acetylcholine and glutamate drive retinal waves in consort) have already demonstrated that acetylcholine is important for the wave spatial extent, whereas glutamate regulates the speed of propagation.

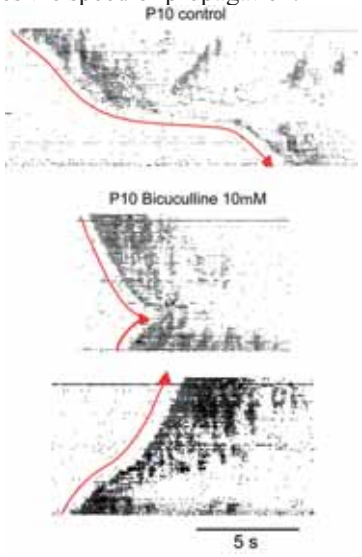

Fig. 4. GABAergic inhibition slows down wave propagation and shortens the duration of the network bursts. Raster plots of spontaneous activity in a P10 retina show that when $GABA_A$ receptors are blocked with bicuculline, waves propagate significantly faster and the bursts are longer.

Here, with the APS MEA, we have shown that indeed, early Stage II cholinergic waves are slow and they propagate over large retinal areas, whereas Stage III glutamatergic waves are faster and spatially more restricted. Stage II waves occur at the time of ocular segregation, when inputs from both eyes compete for a common target, hence requiring synchronization between inputs coming from the same eye. These wide spreading cholinergic waves provide the perfect substrate to achieve this goal. Stage III waves occur at the time of functional map refinement. These faster and spatially more restricted waves provide the perfect substrate for that goal, ensuring coactivation of neighbouring RGCs, hence providing synchronous input to neighbouring cells in their central target. At the same time, however, the clustering and repetitiveness of wave trajectories at Stage III will cause spatially biased neural activity during map refinement, and might therefore interfere with the process of establishing regular ordered retinotopic maps. This novel finding challenges current models of activity-dependent map formation, and calls for a re-investigation of map development at this developmental stage.

Acknowledgement

We thank L. Gasparini at IIT for her help with supplying mouse pups. This work was funded by EPSRC Grant EP/E002331/1 (CARMEN) (ES, SJE), IDEA, FP6-NEST Grant 516432 (LB, AM, MG) and MRC Grant G0900425 (MHH).

References

[1] Sernagor E., Eglen S.J, Wong R.O.L. (2001). Development of retinal ganglion cell structure and function. *Prog Retin Eye Res*, 20, 139-174.

[2] Torborg C.L., Feller M.B. (2005). Spontaneous patterned retinal activity and the refinement of retinal projections. *Prog Neurobiol*, 76, 213–235

[3] Meister M., Wong R.O.L., Baylor D.A., Shatz C.J. (1991). Synchronous bursts of action potentials in ganglion cells of the developing mammalian retina. *Science*, 252, 939-943.

[4] Stafford B.K., Sher A., Litke A.M., Feldheim D.A. (2009) Spatial-temporal patterns of retinal waves underlying activity-dependent refinement of retinofugal projections. *Neuron*, 64, 200-212.

[5] Syed M.M., Lee S., Zheng J., Zhou Z.J. (2004). Stage-dependent dynamics and modulation of spontaneous waves in the developing rabbit retina. *J Physiol*, 560, 533-549.

[6] Zheng J.J., Lee S., Zhou Z.J. (2004). A developmental switch in the excitability and function of the starburst network in the mammalian retina. *Neuron*, 44, 851–864.

[7] Bansal A., Singer J.H., Hwang B.J., Xu W., Beaudet A., Feller M.B (2000). Mice lacking specific nicotinic acetylcholine receptor subunits exhibit dramatically altered spontaneous activity patterns and reveal a limited role for retinal waves in forming ON and OFF circuits in the inner retina. *J Neurosci*, 20, 7672-7681.

[8] Imfeld K., Neukom S., Maccione A., Bornat Y., Martinoia S., Farine P.A., Koudelka-Hep M., Berdondini L. (2008) Large-scale, high-resolution data acquisition system for extracellular recording of electrophysiological activity. *IEEE Trans Biomed Eng*, 55, 2064-2073.

[9] Berdondini L., Imfeld K., Maccione A., Tedesco M., Neukom S., Koudelka-Hep M., Martinoia S. (2009). Active pixel sensor array for high spatio-temporal resolution electrophysiological recordings from single cell to large scale neuronal networks. *Lab Chip*, 9, 2644-2651.

[10] Maccione A., Gandolfo M., Massobrio P., Novellino A., Martinoia S., Chiappalone M. (2008). A novel algorithm for precise identification of spikes in extracellularly recorded neuronal signals. *J Neurosci Meth*, 177, 241-249.

[11] Sernagor E., Young C., Eglen S.J. (2003). Developmental modulation of retinal wave dynamics: shedding light on the GABA saga. *J Neurosci*, 23: 7621-7629.

[12] Sernagor E., Eglen S.J., O'Donovan M.J. (2000). Differential effects of acetylcholine and glutamate blockade on the spatiotemporal dynamics of retinal waves. *J Neurosci*, 20 (RC56), 1-6.

Network oscillation in *rod degenerated (rd1)* retinas

Günther Zeck [1,2*] and Jacob Menzler [1]

1 Department of Computational and Systems Neuroscience, Max Planck Institute of Neurobiology, Martinsried, Germany
2 NMI, Natural and Medical Sciences Institute at the University of Tübingen, Reutlingen, Germany
* Corresponding author. E-mail address: guenther.zeck@nmi.de

1 Introduction

Pathological neuronal oscillations are associated with diverse CNS disorders including neurodegenerative diseases such as Parkinson or epilepsies. They are characterized by enhanced excitability and oscillatory behaviour of the neurons involved. In rod degenerated mouse (*rd1*) retinas gene defects lead to complete blindness. The disease is accompanied by an increased and rhythmic spontaneous activity in the retinal projection neurons [1-3] – the retinal ganglion cells (RGC). Here we assessed the degree of synchronicity between retinal projection neurons and investigated the mechanism underlying the rhythmic discharge.

2 Methods

We recorded extracellular voltages from *in vitro* mouse retinas using a multi-transistor array with 16384 sensors densely packed in 1mm^2. The retinas were isolated from adult *rd1* and *wt* mice (P35-P70) respectively. Extracellular signals attributed to retinal ganglion cell (RGC) action potentials were identified using an appropriate filter range (100 Hz – 10 kHz) and taking advantage of the simultaneous recording on many adjacent electrodes. Local field potentials were detected in the low frequency range (1 – 50 Hz) and analyzed adapting concepts from developmental retinal waves.

3 Results

The majority of RGCs (80% per retinal portion) in rd1 retinas show rhythmic ~10Hz bursting activity. The cross- correlograms between rd1 spike trains display multiple peaks with the central peak randomly shifted with respect to zero lag. RGC spiking is locked to the minima of Local Field Potentials (LFPs) that occur at the same fundamental frequency. LFPs propagate across rd1 retinas at average velocities of 5 – 8 mm/sec. Oscillatory spiking and local field potentials were never encountered in wt retinas.

Inhibition of RGC spiking using TTX abolished RGC spikes but not the LFPs. Inhibitory glycine and GABA-receptor blockers slowed down RGC rhythmicity and the corresponding LFPs. Local field potentials and the concomitant oscillatory spiking disappeared after application of glutamate receptor blockers or after the application of gap junction blockers.

4 Conclusion

Our results indicate that strong excitation - transmitted through a network of electrically coupled interneurons - leads to aberrant large-scale network oscillations. The spatially confined rhythmic activity may explain forms of photopsias reported by blind patients and may help to develop effective treatment strategies for *retinitis pigmentosa*.

References

[1] Ye, J.H. & Goo, Y.S.. *Physiol. Measurement* **28**, 1079-1088 (2007)
[2] Stasheff, SF et al.. *J. Neurophysiol* **99,** 1408 - 1421 (2008)
[3] Margolis, D.J., et al. *J. Neurosci* **28**, 6526- 6536 (2008).

Spatial and Temporal Patterns and Information Processing in Retinal Neurons

Liang Pei-Ji*, Jing Wei, Liu Wen-Zhong, Gong Hai-Qing, Zhang Pu-Ming

School of Life Sciences and Biotechnology, Shanghai Jiao Tong University, Shanghai, China
* Corresponding author. E-mail address: pjliang@sjtu.edu.cn

The spike activities of bullfrog retinal ganglion cells in response to different visual patterns were recorded using multi-electrode array, and relevant spatio-temporal properties of the retinal ganglion cells activities in response to the visual stimulation were characterized. The adaptation properties were also examined.

1 Background

The first stage for visual information processing in vertebrates occurs in the retina. However, the retinal function is constrained by a number of factors such as the anatomic limitation, the metabolic limitation, and the noise in the neural circuitry. Our research is mainly focused to investigate the reliability and efficiency of information processing of the retinal neurons under such limitations and the related spatial and temporal patterns of the neural activities. In the present study, the spike activities of bullfrog retinal ganglion cells in response to different visual patterns were recorded using multi-electrode array, and relevant spatio-temporal properties of the retinal ganglion cells activities in response to the visual stimulation were characterized. The adaptation properties were also examined.

2 Method

Spikes from bullfrog retinal ganglion cells were recorded by MEA electrodes (8×8, MMEP-4, CNNS UNT, USA) using a commercial multiplexed data acquisition system with a sampling rate of 40 kHz (MEA workstation, Plexon Inc. Texas, USA). Light stimulus was generated from a computer monitor (Iiyama, Vision Master Pro 456, Japan) and was focused to form a 1.1 × 1.1 mm2 image on the isolated retina via a lens system. The stimulation protocols were: (1) Checker-board stimulus consisted of 8×8 sub-squares, with each sub-square covering an area of 132×132 μm2 on the retinal piece and was assigned randomly with a value either “1” (white light, 77.7 nW/cm2) or “0” (dark, 0 nW/cm2); (2) Grating (horizontal or vertical) stimuli consisted of light bars (77.7 nW/cm2) and dark bars (0 nW/cm2), with the width of each bar being 177 μm when projected on the retina.

3 Results

In the present study, an analytical tool based on measurement of subsequence distribution discrimination (MSDD) [1,2] analysis was applied to deal with a group of spike train sequences and analyze the spatio-temporal pattern of concerted activities among the neurons. The analytical results show that: (1) In our experimental protocols, each single ganglion cell’s firing rate did not change much during its responses elicited by different stimulation pattern; (2) During adaptation to any particular visual pattern, the neuronal firing activities was gradually reduced; (3) By applying MSDD, the spatio-temporal patterns of the neuronal activities in response to different visual patterns were identifiable.

4 Conclusion

The results show that the population adaptation process follows the single neuronal adaptation process in a sense that the neuronal activities were gradually reduced, but the spatio-temporal patterns of population neuronal activities were identifiable, which served for reliable and efficient information processing.

Acknowledgement

This work was supported by the grant from National Basic Research Program of China under Grant No. 2005CB724301.

References

[1] Fang W.W., Roberts F.S., Ma Z. R. (2001) A measure of discrepancy of multiple sequences. *Information Science*, 137, 75-102.

[2] Wang G.L., Liu X., Zhang P.M., Liang P. J. (2006) A new method for multiple spike train analysis based on information discrepancy. *LNCS*, 4232, 30-38.

Recording of Neural Activity of Mouse Retinal Ganglion Cells by Means of an Integrated High-Density Microelectrode Array

Michele Fiscella[1], Urs Frey[2], David Jäckel[1], Jan Müller[1], Ralf Streichan[1], Ian L. Jones[1], Branka Roscic[1], Karl Farrow[3], Botond Roska[3], Andreas Hierlemann[1].

1 Bio Engineering Laboratory, ETH Zurich, Basel, Switzerland.
2 Bio Engineering Laboratory, ETH Zurich, Basel, Switzerland; now at IBM Research, Zurich, Switzerland.
3 Neural Circuits Laboratory, Friedrich Miescher Institute, Basel, Switzerland.

Retinal ganglion cells form the output layer of the retina and send the encoded visual information to the brain. Using a high-density microelectrode array to scan the ganglion cell layer, we were able to sort the spiking activity of different units and select a defined subset of electrodes to record from a specific group of retinal ganglion cells.

1 Background/Aims

The mammalian retina extracts specific features from the visual input. The final output is computed in the ganglion cell layer and consists of complex spatio-temporal patterns of action potentials [1]. Microelectrode-array (MEA) technology is an ideal tool for recording spike trains of retinal ganglion cell populations.

Here we show the possibility to scan the ganglion cell layer and record the activity of potentially every active retinal ganglion cell on the array.

2 Methods

We used a complementary metal-oxide-semiconductor (CMOS)-based MEA (Fig. 1) providing high spatio-temporal resolution and high signal-to-noise ratio to record neural activity from mouse retinal ganglion cells.

The MEA features 11,011 metal electrodes, placed in an area of 2.0x1.75 mm^2 (126 electrodes at arbitrary positions can be selected for synchronous recording). Each platinum electrode has a diameter of 7 μm, and the center-to-center distance between the electrodes is 17 μm. Flexibility in the electrode selection is attained through an analog switch matrix located underneath the electrode array [2].

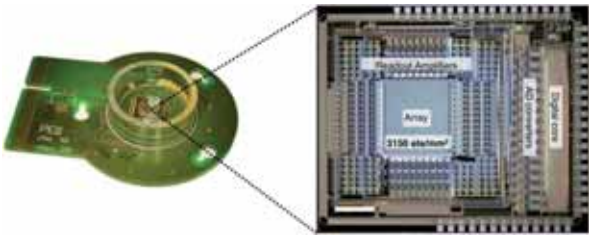

Fig. 1. Packaged high-density MEA device and overall chip micrograph. Scale bar: 1 mm.

The retinae were isolated at ambient light from the C3H/HeNCrl (*rd1*) mouse strain at P80 in Ringer's medium (in mM: 110 NaCl, 2.5 KCl, 1 $CaCl_2$, 1.6 $MgCl_2$, 10 D-glucose, 22 NaHCO3, bubbled with 5% CO_2/95% O2). Once a piece of the retina was isolated, it was placed with the ganglion cell side contacting the MEA. The retina was held on the array by a custom-built holder and superfused with Ringer's medium at 36° C.

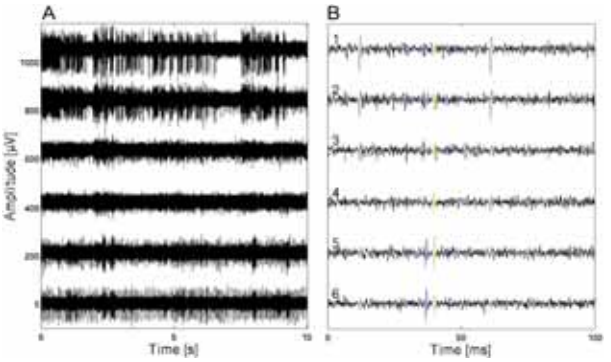

Fig. 2. (A) | Recordings from *rd1* mouse retinal ganglion cells. **(B)** | Zoom into (A) with spikes from 3 units identified after spike sorting and marked in different colors. Note: each unit is detectable on more than one electrode.

3 Results

We used the *rd1* mouse retina to record spontaneous activity [3] from retinal ganglion cells. Action potentials from single ganglion cells were simultaneously recorded on several electrodes (Fig. 2). The highly redundant information provided by our system allows us to use independent-component analysis (ICA) for spike sorting [2]. In most cases we measured somatic signal with amplitudes between 100-300 μV (Fig. 3). In several cases, we were able to measure the propagation of corresponding axonal signals.

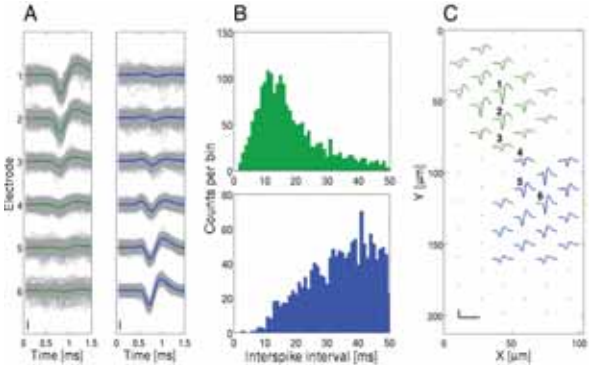

Fig. 3. (A) | Superimposition of events for the green and blue units detected in Fig. 2B during 2 min recording. The averaged signal is marked in color. Scale bar: 50 µV. **(B)** | Inter-spike interval histograms; **(C)** | RGCs footprints. Scale bar: 50 µV, 1.5 ms

After spike sorting, the spatial position of each ganglion cell can be determined. Consequently, it is possible to select 2-4 electrodes directly underneath any ganglion cell of interest. The electrodes are chosen in a way to most efficiently separate the signal of the cell of interest from those of the surrounding cells (Fig. 4).

The large flexibility in the electrode selection along with the high electrode density is important for two reasons: (1) our system allows to rapidly scan large areas of the ganglion cell layer (2) we can potentially record activity from every ganglion cell on the array (Fig. 5).

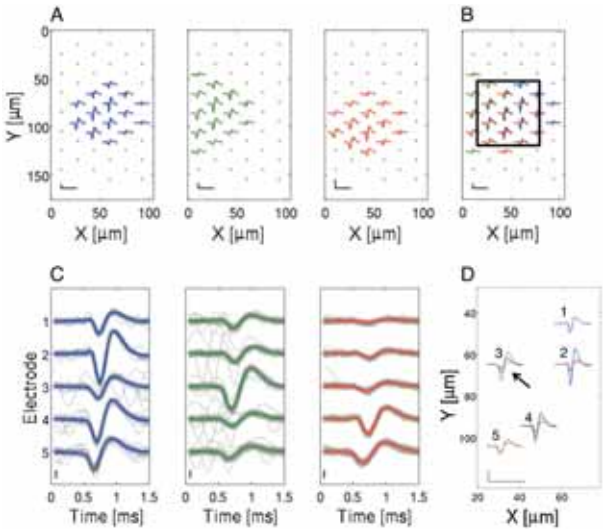

Fig. 4. (A) | Footprints of 3 neighboring cells. Scale bar: 100 µV, 1.5 ms. **(B)** | Same cells as in (A) but plotted together. Note the high degree of overlap between the footprints. Scale bar 100 µV, 1.5 ms. **(C)** | Superimposition of events from units in (A) on 5 electrodes inside the black rectangle in (B). Scale bar 50 µV. **(D)** | The electrode providing best identification of the green cell is indicated by the black arrow. Scale bar 100 µV, 1.5 ms.

4 Conclusions

The integrated CMOS-based MEA offers the possibility to rapidly scan large retina patches, to identify consistently spiking units, and to record from

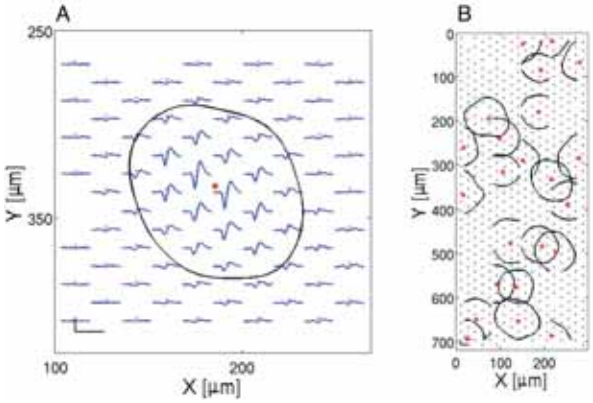

selected cells of the ganglion cell layer. This strategy will enable us to record light-evoked activity from functionally identified RGCs in their network context.

Fig. 5. (A) | RGC footprint. The red dot indicates the electrode with the highest spike amplitude. The black contour line represents an equipotential line at half peak amplitude. Scale bar: 100 µV, 1.5 ms. **(B)** | RGCs sorted from different overlapping recording blocks, represented in the same way as in (a).

Acknowledgement

This work was supported by the Swiss Initiative in Systems Biology, SystemsX.ch, with an interdisciplinary PhD grant.

References

[1] Wassle H. Parallel processing in the mammalian retina. *Nat Rev Neurosci*. 2004;**5**:747-57.

[2] Frey U, Egert U, Heer F, Hafizovic S, Hierlemann A. Microelectronic system for high-resolution mapping of extracellular electric fields applied to brain slices. *Biosens Bioelectron*. 2009;**24**:2191-8.

[3] Stasheff SF. Emergence of sustained spontaneous hyperactivity and temporary preservation of OFF responses in ganglion cells of the retinal degeneration (rd1) mouse. *J Neurophysiol*. 2008;**99**:1408-21.

Electrical response of rabbit retinal ganglion cells and their intraretinal conduction after optic nerve crush

Christian Leibig[1*], Günther Zeck[2*]

1 Membrane- and Neurophysics, Max Planck Institute for Biochemistry, Martinsried
2 Computational- and Systems Neurobiology, Max Planck Institute of Neurobiology Martinsried, Germany
* Corresponding authors. E-mail addresses: zeck@neuro.mpg.de, leibig@biochem.mpg.de

The optic nerve represents an ideal model to study the degeneration and regeneration of CNS axons after either crush or section.
Here we investigate electrophysiological properties in the rabbit retina following optic nerve crush (ONC). The rabbit retina was selected because we were able to measure intraretinal propagation of individual action potentials at very high spatial (7.8 µm) and temporal (0.1 msec) resolution using a multi-transistor array comprising 16384 extracellular sensor sites. In addition we quantified spontaneous activity and response latencies to flashed spots in populations of retinal ganglion cells from the same retina. Retinas were isolated at three time points following optic nerve crush: after 4, 7 and 14 days respectively.
Intraretinal conduction velocity did not change significantly in retinas isolated four days after ONC compared to control velocities (mean 1.3 m/sec). The average intraretinal velocity dropped to 1.1 m/sec in axons isolated 7 days (n = 14) and 14 days after ONC (n=14).
The median spontaneous firing rate (6 Hz) measured under otherwise identical conditions did not change after optic nerve crush. However, we found in each of the three post-crush conditions cells with firing rates exceeding 30 Hz - a feature not detected in control retinas. The average response latency to flashed spots (mean: 55 ms, n = 40 ON cells per retina) did not change after optic nerve crush.
Our results indicate that two weeks after optic nerve crush intraretinal conduction is reduced but the circuitry presynaptic to the ganglion cells remains functional.